GSA Data Repository 2017329

"Fault gouge graphitization as evidence of past seismic slip"

Li-Wei Kuo*, Fabio Di Felice, Elena Spagnuolo, Giulio Di Toro, Sheng-Rong Song, Stefano Aretusini, Haibing Li, John Suppe, Jialiang Si, Cheng-Yen Wen

*To whom correspondence should be addressed. Email: liweikuo@ncu.edu.tw

This file includes texts, figures and tables that are divided into five data repository items:

Data repository Item DR1: FIB-TEM-EDS analyses on starting materials and experimental products

Data repository Item DR2: Summary of the experiments performed with the rotary shear apparatus SHIVA

Data repository Item DR3: Computation of temperature evolution in the principal slipping zone

Data repository Item DR4: Description of method of Raman spectroscopy and peak decomposition of Raman spectra

Data repository Item DR5: Spectra decomposition on Raman results of WFSD-1 materials

Data repository Item DR6: Spectra decomposition on Raman results of rock friction experiment products

Data repository Item DR1

FIB-TEM-EDS analyses on starting materials and experimental products

The specimen for transmission electron microscopy (TEM) was prepared using a focused ion beam (FIB) system, FEI Helios 600i. A thin piece of the sample of 10 μm (length) by 4 μm (height) was cut with a gallium ion beam in the FIB system and lifted off using an *in-situ* manipulator. The specimen was mounted on a Cu supporting washer, and further thinned down to less than 100 nm. The electron transmission investigations were with the JEOL 2010F field emission TEM system. The accelerating voltage of the electron beam was 200 KV. Bright-field TEM images were captured. Selected-area electron diffraction (SAED) patterns were taken using the selected-area aperture to obtain the electron diffraction pattern of the principle slip zone (PSZ).

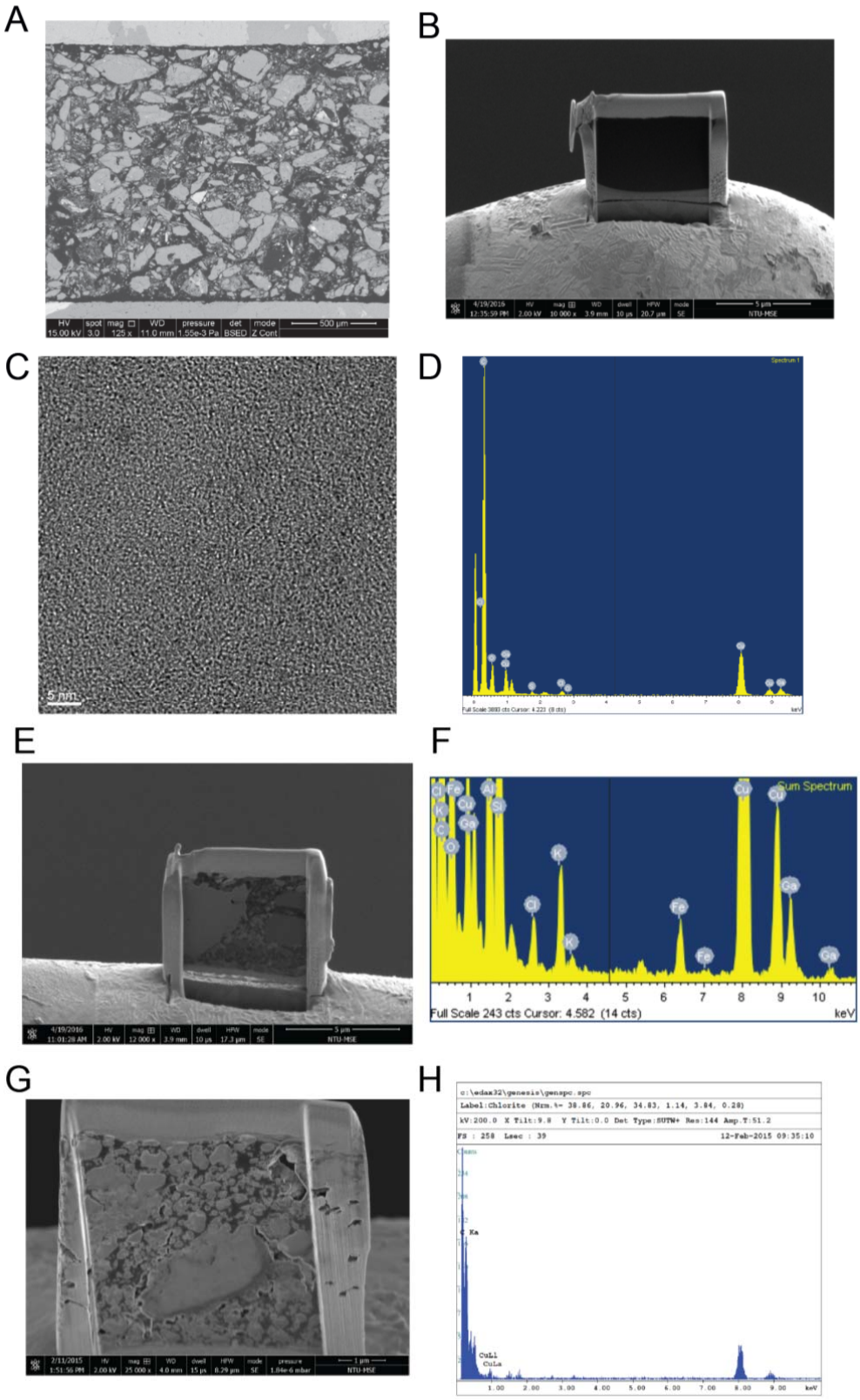

Figure DR01: FIB-TEM-EDS analyses on starting material and products at sub-seismic and seismic rates. (a) SEM image of the starting material with carbon grains (black in color ranging from

tens to hundreds micrometers in size) are well-distributed. (b) The carbon grain cut from the starting material with the FIB method. (c and d) TEM image and EDS spectrum of poorly order carbon found in the starting material. The presence of gallium ion in the spectrum is the due to TEM lamella sample preparation. (e) Lamella of the PSZ of the gouge sheared at sub-seismic rates (s1090) cut with the FIB method. (f) TEM-EDX of the gouge sheared at sub-seismic slip rates: the selected area includes carbon (53.50 wt.%, main element), plus copper (18.80 wt.%, TEM grid), oxygen (12.41 wt.%), silicon (8.44 wt.%), aluminum (3.67 wt.%), gallium (1.3 wt.%, due to sample preparation), and potassium (0.86 wt.%), chloride (0.38 wt.%), and iron (0.64 wt.%). (g) The FIB lamella of the PSZ of the gouge sheared at seismic rates (s1002). (h) TEM-EDX of the gouge sheared at seismic slip rate (s1002): the analyzed grain (also shown in Fig. 4d) is mainly made by carbon (96.4 wt.%). The presence of copper (3.6 wt.%) is due to TEM grid.

Data repository Item DR2

Table DR2: Summary of the experiments performed with the rotary shear apparatus SHIVA

Experimental condition for nine friction experiments performed on fault gouge layers at room-temperature and room-humidity. Selected friction tests are plotted in Fig.2 of the main text. σ_n: normal stress; τ_{ss}: steady-state shear stress; Frictional power density: $\tau_e \cdot V$; Friction work: $\tau_{ss} \cdot d$

Experiment	σ_n (MPa)	τ_{ss} (MPa)	Slip velocity V (m/s)	Frictional power density (MW/m^2)	Acceleration and deceleration (m/s^2)	Frictional work (MJ/m^2)	Total slip d (m)	Ambient condition (RH: Room-humidity WD: Water-damped)
s1002	8.5	1.4	3	4.2	6	4.2	3	RH
s1079	8.5	1.6	3	4.8	6	4.8	3	RH
s1090	8.5	4.9	0.0003	0.00147	6	14.7	3	RH
s1093	8.5	4.8	0.0003	0.00144	6	14.4	3	RH
s1104	8.5	3.1	0.0003	0.00093	6	6.82	2.2	WD
s1105	8.5	1.3	3	3.9	6	3.9	3	WD
s1108	8.5	1.8	3	5.4	6	5.4	3	RH
s1111	8.5	3.3	0.0003	0.00099	6	7.26	2.2	WD
s1337	8.5	1.4	3	4.2	6	4.2	3	WD

Data repository Item DR3

Computation of temperature evolution in the principal slipping zone

A finite element methods thermo-mechanical model was performed with COMSOL Multiphysics® software to calculate the frictional heat produced during the experiments and the associated temperature evolution in the gouge and sample holder system (see [*Kitajima et al.*, 2010]).

The model considers a heat transfer model by thermal conduction. Temperatures are calculated as function of time, in correspondence of the equivalent radius position (ca. halfway between inner and outer radiuses of the gouge layer). This temperature was named T_{eq} in previous works [e.g., *Kitajima et al.*, 2011].

The geometry of the sample assemblage of SHIVA was fully reproduced, including the shape and the type of material of the different domains (gouge, steel, etc.). The mesh was triangular, with element size of <250 μm in the gouge domain and <1.25 mm in the steel domains. Thermal properties are summarized in Table 1 for: gouge, ALSI304 steel and tungsten carbide.

	Gouge	ALSI304	Tungsten carbide
Thermal conductivity, k (W/mK)	3	16	69 (up to 800K, then f(T))
Thermal capacity, Cp (J/kgK)	800	500	180 (293K), then f(T)
Density (kg/m3)	2500	8000	15770.0

The following experimental data are imported in the model: i) the total torque measured during the experiment $M(t)$, and ii) the equivalent velocity $v_{eq}(t)$. We calculated: i) the shear resistance of the gouge $\tau(t)$ (Equation 1), ii) the equivalent velocity $v_{eq}(t)$, and converted in angular velocity $\omega(t)$ (Equation 2) to calculate then the tangential velocity v(r,t) (Equation 3).

$$\tau(t) = (3*M(t)*0.736*10^6)/(2*\pi*(r_o\text{^}3-r_i\text{^}3)) \quad \text{Eq. 1}$$

$$\omega(t) = v_{eq}(t)/(4/3*\pi*(r_i\text{^}2+r_i*r_o+ro\text{^}2)/(ri+ro)) \quad \text{Eq. 2}$$

$$v_{eq}(r,t) = 2\pi*\omega(t)*r \quad \text{Eq. 3}$$

Where r_i and ro are the inner and outer radius of the gouge ring (0.0175 and 0.0275 m, respectively). Shear resistance τ and tangential velocity v_{eq} (r,t) are calculated after [*Shimamoto and Tsutsumi*, 1994].

The heat source (W/m^2) was positioned as sketched in (Figure DR03) and calculated according to:

$$Q = \tau(t)* v_{eq}(r,t) \quad \text{Eq. 4}$$

The position of Q is at the boundary between gouge layer and steel, differently from previous studies where heat sources were located inside the gouge layer [*Kitajima et al.*, 2010; *French et al.*, 2014]. We chose this heat source position because of microstructural evidences of heat and strain localization along this interface.

References

French, M. E., H. Kitajima, J. S. Chester, F. M. Chester, and T. Hirose (2014), Displacement and dynamic weakening processes in smectite-rich gouge from the Central Deforming Zone of the San Andreas Fault, *J. Geophys. Res. Solid Earth*, *119*(3), 1777–1802, doi:10.1002/2013JB010757.

Kitajima, H., J. S. Chester, F. M. Chester, and T. Shimamoto (2010), High-speed friction of disaggregated ultracataclasite in rotary shear: Characterization of frictional heating, mechanical behavior, and microstructure evolution, *J. Geophys. Res. Solid Earth*, *115*, 1–21, doi:10.1029/2009JB007038.

Kitajima, H., F. M. Chester, and J. S. Chester (2011), Dynamic weakening of gouge layers in high-speed shear experiments: Assessment of temperature-dependent friction, thermal pressurization, and flash heating, *J. Geophys. Res.*, *116*(B8), doi:10.1029/2010JB007879.

Shimamoto, T., and A. Tsutsumi (1994), A new rotary-shear high-speed frictional testing machine: its basic design and scope of research, *J. Tecton. Res. Group Jpn.*, *39*, 65–78.

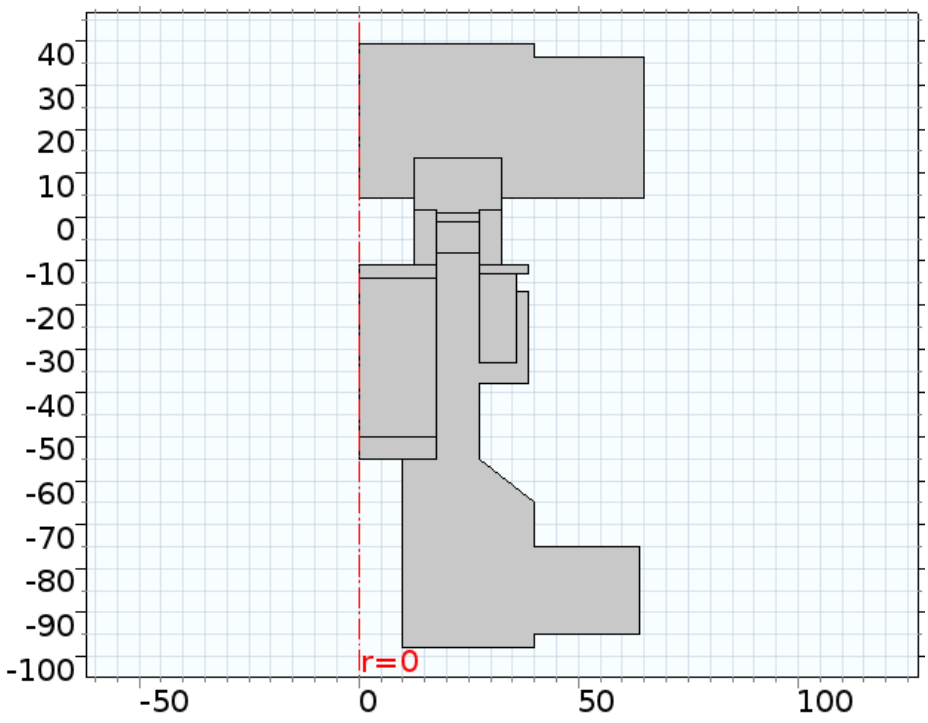

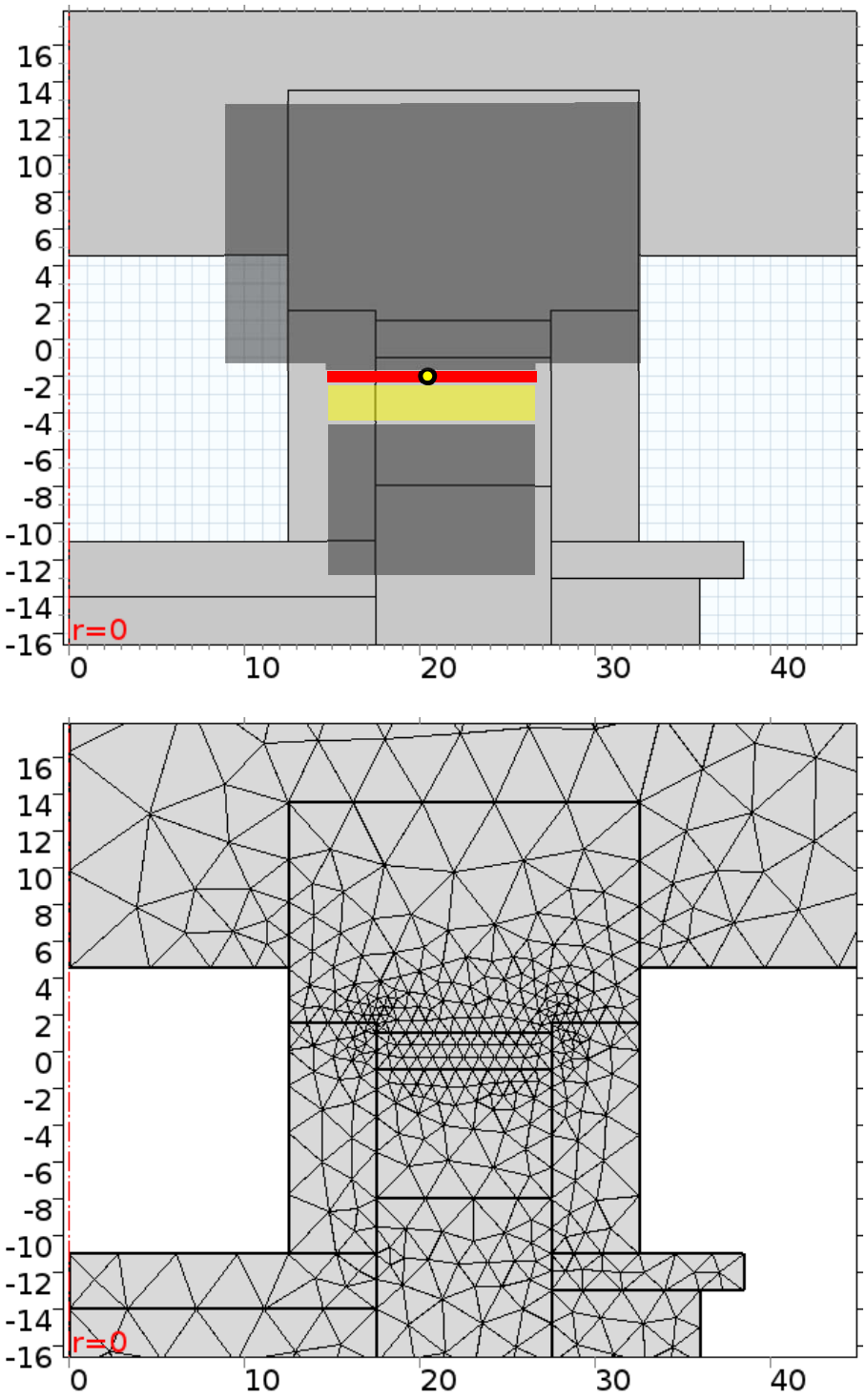

Figure DR03. a) Geometry of the model, b) Zoom with highlighted the positions of the heat source (red line) and of the point where output temperature was calculated (yellow spot); materials are overlaid: gouge (yellow), tungsten carbide (dark grey), AISI304 steel (grey); c) Geometry of the model with overlaid model mesh.

Data repository Item DR4

Description of method of Raman spectroscopy and peak decomposition of Raman spectra

The Raman spectra of carbonaceous materials were directly measured on powder with a Horiba Jobin Yvon UV-VIS Labram HR Micro-Raman spectrometer at the National Taiwan Museum, Taiwan, and with the *Thermofisher* un-polarized apparatus at the department of Chemistry at Padua university, Italy. A green laser monochromatic light (wavelength 580 nm) was used as the excitation source and beam size was 1-2 μm with a ×50 objective, with a final laser power of 5 mW at sample surface. Acquisition time was 2 seconds and 5 spectra were measured for each sample. Peak analysis was performed using the commercial software PeakFit 4.12 (Systat Software, Inc.) and the following parameters were calculated: peak intensity, peak width (at half maximum), and peak position (frequency). Peak profiles were fitted using a pseudo-Voigt function (Gaussian-Lorentzian linear combination) (Sadezky et al., 2005; Furuichi et al., 2015). Peak analysis was done with an excitation beam of wavelength of 532 nm and focused in the 1100-1800 cm^{-1} region of the Raman spectrum which includes the first-order bands of CM: the G (from 1575 cm^{-1} - 1592 cm^{-1}), the D1 (from 1330 cm^{-1} - 1336 cm^{-1}) and the D3 (from 1490 cm^{-1} - 1525 cm^{-1}) bands (Fig. 1b inset in the main text).

For the natural fault samples, we analyzed clay-sized fraction carbon deposited on glass slides (Si et al., 2014). For each sample, ten analyses were taken and then all the spectral parameters were averaged (Fig.1b and c). For the experimental products, we analyzed the strain localization zone of the gouge layer. For each deformed sample, fourteen analyses were taken and then all the spectral parameters were averaged (bigger solid shapes in Fig.3; DR5).

References

Sadezky, A., Muckenhuber, H. Grothe, H., Niessner, R., and U. Poschl U., 2005. Raman microspectroscopy of soot and related carbonaceous materials: Spectral analysis and structural information. Carbon 43, p. 1731-1742.

Furuichi, H., Ujiie, K., Kouketsu, Y., Saito, T., Tsutsumi, A., and Wallis, S., 2015. Vitrinite reflectance and Raman spectra of carbonaceous material as indicators of frictional heating on faults: Constraints from friction experiments. Earth Planet. Sci. Lett. 424, p. 191-200, doi:10.1016/j.epsl.2015.05.037.

Data repository Item DR5

Table DR5: Results of spectra decomposition along the WFSD-1 drilling depths for breccia and gouge of the Longmenshan fault zone.

Type	Depth (m)	D1/G Intensity	D1/G Width ratio	Peak position (cm^{-1})		Gouge or Breccia /average Breccia	
				D1	G	D1	G
Breccia	588.69	0.93	1.46	1336	1579.7	1.02	1
Breccia	588.78	0.93	1.51	1334.8	1581.9	1.01	0.96
Breccia	588.82	0.95	1.47	1333.5	1577.8	1.05	1.02
Gouge	588.88	0.84	1.66	1332	1590.4	0.93	0.80
Gouge	588.98	0.86	1.67	1333.3	1590	0.94	0.80
Gouge	589.05	0.79	1.46	1334.1	1588.6	0.86	0.84
Gouge	589.12	0.73	1.54	1331.6	1588.3	0.90	0.84
Gouge	589.19	0.76	1.54	1332.2	1590.8	0.91	0.85
Gouge	589.22	0.75	1.63	1331.9	1590.8	0.90	0.79
Gouge	589.25	0.80	1.55	1335.3	1589	0.93	0.86
Breccia	589.32	0.95	1.49	1334.3	1578.6	1.06	1.02
Breccia	589.42	0.90	1.4	1332.9	1575.1	1.02	1.04

Data repository Item DR6

Table DR6: Results of spectra decomposition for one starting material and four experimental products performed at both almost sub-seismic and seismic rates and at room-humidity (RH) and water-damped (WD) conditions.

Sample	Experimental conditions	D1/G Intensity	D1/G Width ratio	Peak position (cm^{-1})		experiment /average starting material	
				D1	G	D1	G
starting material	RH	1.08	1.86	1334	1571	1	1
s1002	3 m/s, RH	0.9	2.68	1334	1591.8	0.98	0.68
s1090	0.0003 m/s, RH	0.74	3.05	1338	1604	1.1	1.05
s1104	0.0003 m/s, WD	0.76	2.78	1335	1603	0.99	1.03
s1105	3 m/s, WD	0.72	2.77	1331	1602	0.95	1.01